J Stat Phys (2017) 167:1–13
DOI 10.1007/s10955-017-1730-1

Complex Singular Solutions of the 3-d Navier–Stokes Equations and Related Real Solutions

Carlo Boldrighini[1] · **Dong Li**[2] · **Yakov G. Sinai**[3]

Received: 25 November 2016 / Accepted: 20 January 2017 / Published online: 6 February 2017

Abstract By applying methods of statistical physics Li and Sinai (J Eur Math Soc 10:267–313, 2008) proved that there are complex solutions of the Navier–Stokes equations in the whole space $\mathbb{R}^3$ which blow up at a finite time. We present a review of the results obtained so far, by theoretical work and computer simulations, for the singular complex solutions, and compare with the behavior of related real solutions. We also discuss the possible application of the techniques introduced in (J Eur Math Soc 10:267–313, 2008) to the study of the real ones.

Keywords Navier–Stokes equations · Global regularity · Blow-up

1 Introduction

The present paper is intended to be a review of the results obtained in recent years on the behavior of a class of complex solutions of the Navier–Stokes equations in the whole space $\mathbb{R}^3$, which exhibit a singularity ("blow-up") at a finite-time. They were first introduced by Li and Sinai in 2008 [8], as a contribution to the long-lasting problem on the existence of singular

Partially supported by INdAM (G.N.F.M.) and M.U.R.S.T. research funds.

✉ Carlo Boldrighini
boldrigh@mat.uniroma1.it

Dong Li
mpdongli@gmail.com

Yakov G. Sinai
sinai@math.princeton.edu

1 Istituto Nazionale di Alta Matematica (INdAM), GNFM, Unità locale Università Roma Tre, Largo S. Leonardo Murialdo, 1, 00146 Rome, Italy

2 Department of Mathematics, University of British Columbia, 1984 Mathematics Road, Vancouver, BC V6T 1Z2, Canada

3 Department of Mathematics, Princeton University Princeton, New Jersey, NJ 08544, USA

solutions. The approach is based on techniques which are typical of Statistical Physics, such as the Renormalization Group Method.

Our review is based both on theoretical work and computer simulations. We will also discuss the behavior of related real solutions, as revealed by computer simulations, and discuss the perspectives of applying to them the techniques introduced in [8].

The modern mathematical theory of the Navier–Stokes equations begins in 1934 with a paper of Jean Leray [7]. Since then, one of the main open questions is whether the solution for smooth initial data and in absence of external forces can become singular in a finite time. This is the celebrated *global regularity problem*, which is also one of the seven Millennium Open Problems of the Clay Mathematical Institute. [It refers, of course, only ro real solutions of the Eq. (1)].

Leray proved an existence theorem for all times, and, as regularity can be proved, in general, only for finite times, he was led to believe that the singular solutions do exist and the loss of regularity and uniqueness is related to the turbulent behavior. Modern ideas on turbulence are not related to singularities, but the possible singular solutions, on which we now have much more information than at the time of Leray, could describe phenomena such as hurricanes, which appear as a sudden concentration of energy in a finite space region. There is at present no effective model describing such phenomena, and we know in fact [11] that a loss of smoothness implies the divergence of the solution at some point of the physical space.

Much work has been devoted to the global regularity problem, both theoretical and by computer simulations. In the last decade proofs of a finite-time blow-up were obtained for some variants of the dyadic model of Katz and Pavlovic [4,6], a discrete simplification of the Navier–Stokes equations which preserves energy conservation.

An important result, inspired by the dyadic model, was recently obtained by T. Tao [12], who proved the existence of finite-time blow-up for a modified Navier–Stokes system, which also satisfies the energy conservation. The modification consists in replacing the bilinear term, which is responsible for the energy transfer to the high Fourier modes, with a suitable average. The introduction of the paper of Tao is also an excellent review of the present state of the global regularity problem.

As for computer simulations, reliable evidence for a blowup is difficult to obtain. Simulations of the three-dimensional Navier–Stokes equations are computationally onerous and the flow is unstable for high values of the velocity and the vorticity. In absence of a theoretical guideline computation is hopeless. For an appreciation of the situation we refer the reader to the paper [5].

We consider the Navier–Stokes system in $\mathbb{R}^3$ for smooth initial data, with no boundary conditions and in absence of external forces

$$\frac{\partial \mathbf{u}}{\partial t} + \sum_{j=1}^{3} u_j \frac{\partial}{\partial x_j}\mathbf{u} = \Delta \mathbf{u} - \nabla p, \qquad \mathbf{x} = (x_1, x_2, x_3) \in \mathbb{R}^3. \tag{1}$$

$$\nabla \cdot \mathbf{u} = 0, \qquad \mathbf{u}(\cdot, 0) = \mathbf{u}_0.$$

Here p is the pressure and we assume for the viscosity $\nu = 1$ (which is always possible by rescaling). Following Li and Sinai [8] the problem (1) is reformulated as a convolution integral equation by introducing the modified Fourier transform

$$\mathbf{v}(\mathbf{k}, t) = \frac{i}{(2\pi)^3} \int_{\mathbb{R}^3} \mathbf{u}(\mathbf{x}, t) e^{i\langle \mathbf{k}, \mathbf{x}\rangle} d\mathbf{x}, \qquad \mathbf{k} = (k_1, k_2, k_3) \in \mathbb{R}^3, \tag{2}$$

where $\langle \cdot, \cdot \rangle$ denotes the scalar product in $\mathbb{R}^3$. By a Duhamel formula the Navier–Stokes system goes into an integral equation for the complex vector $\mathbf{v}(\mathbf{k}, t)$:

$$\mathbf{v}(\mathbf{k}, t) = e^{-t\mathbf{k}^2}\mathbf{v}_0(\mathbf{k}) +$$

$$+ \int_0^t e^{-(t-s)\mathbf{k}^2} ds \int_{\mathbb{R}^3} \langle \mathbf{v}(\mathbf{k} - \mathbf{k}', s), \mathbf{k} \rangle P_{\mathbf{k}} \mathbf{v}(\mathbf{k}', s) d\mathbf{k}', \tag{3}$$

where $\mathbf{v}_0$ is the transform of $\mathbf{u}_0$, and $P_{\mathbf{k}}$ is the solenoidal projector expressing incompressibility

$$P_{\mathbf{k}}\mathbf{v} = \mathbf{v} - \frac{\langle \mathbf{v}, \mathbf{k} \rangle}{\mathbf{k}^2}\mathbf{k}.$$

The real solutions of the integral Eq. (3) correspond in general to complex solutions $\mathbf{u}(\mathbf{x}, t)$. Real solutions of (3) corresponding to real fluid flows are obtained if the initial data $\mathbf{v}_0(\mathbf{k})$ is odd in $\mathbf{k}$.

In the paper [8] it was proved, with techniques inspired by the Renormalization Group Method, that there is a class of real solutions of the integral Eq. (3) which blow up at a finite time. They correspond to complex solutions $\mathbf{u}(\mathbf{x}, t)$ in $\mathbf{x}$-space, and do not conserve energy (more precisely, the energy identity holds but it is not coercive). In fact the total energy diverges at the critical time. In spite of the fact that they are unphysical, their existence and their behavior are important features of the NS equations, which has consequences for the real solutions.

In fact, some of their properties, concerning especially the enhancement of the high $\mathbf{k}$-modes, are in part inherited by the real solutions obtained by anti-symmetrizing the initial data. Although it is unclear whether such real solutions can become singular, it appears that the methods introduced in the paper [8] can be extended to them, and thereby provide some insight on a class of real fluid flows of which we do not know much.

A remarkable fact for the solutions introduced in [8] is that they have a rather simple structure in $\mathbf{k}$-space near the critical time, which gives insight on their behavior, and greatly simplifies the computer simulations.

The plan of the paper is as follows. In Sect. 2 we review the main rigorous results so far obtained on the complex solutions introduced in [8], with some hints of the proofs, whenever possible. For the full proofs we refer the reader to the literature in quotation.

In Sect. 3 we discuss some open problems on the behavior of the singular complex solutions, with indications on the scope of further mathematical research, supported by the results of recent computer simulations.

The concluding section deals with real-valued solutions which inherit some features of the complex solutions. It is a new class of flows of real fluids, which, as shown by computer simulations, exhibit an interesting behavior. We present some results from computer experiments and briefly discuss possible applications of the methods introduced in [8] in order to get rigorous results.

2 Blow-up of Complex Solutions Represented as Power Series

We begin by reviewing the approach and the main results of the paper [8].

Multiplying the initial data $\mathbf{v}_0$ by a positive parameter A and iterating the Duhamel formula we can write the solution as a power series

$$\mathbf{v}_A(\mathbf{k},t) = Ae^{-t\mathbf{k}^2}\mathbf{v}_0(\mathbf{k}) + \int_0^t e^{-\mathbf{k}^2(t-s)} \sum_{p=2}^{\infty} A^p \mathbf{g}^{(p)}(\mathbf{k},s)ds. \tag{4}$$

Substituting into the equation, and setting $\mathbf{g}^{(1)}(\mathbf{k},s) = e^{-s\mathbf{k}^2}\mathbf{v}_0(\mathbf{k})$, we see that

$$\mathbf{g}^{(2)}(\mathbf{k},s) = \int_{\mathbb{R}^3} \left\langle \mathbf{v}_0(\mathbf{k}-\mathbf{k}'),\mathbf{k}\right\rangle P_{\mathbf{k}}\mathbf{v}_0(\mathbf{k}')e^{-s(\mathbf{k}-\mathbf{k}')^2 - s(\mathbf{k}')^2}d\mathbf{k}',$$

and for $p > 2$ the functions $\mathbf{g}^{(p)}(\mathbf{k},s)$ satisfy the recursive relation

$$\begin{aligned}
&\mathbf{g}^{(p)}(\mathbf{k},s)\\
&= \int_0^s ds_2 \int_{\mathbb{R}^3} \left\langle \mathbf{v}_0(\mathbf{k}-\mathbf{k}'),\mathbf{k}\right\rangle P_{\mathbf{k}}\mathbf{g}^{(p-1)}(\mathbf{k}',s_2)e^{-s(\mathbf{k}-\mathbf{k}')^2-(s-s_2)(\mathbf{k}')^2}d\mathbf{k}'\\
&+ \sum_{\substack{p_1+p_2=p\\ p_1,p_2>1}} \int_0^s ds_1 \int_0^s ds_2 \int_{\mathbb{R}^3} \left\langle \mathbf{g}^{(p_1)}(\mathbf{k}-\mathbf{k}',s_1),\mathbf{k}\right\rangle\\
&\cdot P_{\mathbf{k}}\mathbf{g}^{(p_2)}(\mathbf{k}',s_2)e^{-(s-s_1)(\mathbf{k}-\mathbf{k}')^2-(s-s_2)(\mathbf{k}')^2}d\mathbf{k}'\\
&+ \int_0^s ds_1 \int_{\mathbb{R}^3} \left\langle \mathbf{g}^{(p-1)}(\mathbf{k}-\mathbf{k}',s_1),\mathbf{k}\right\rangle P_{\mathbf{k}}\mathbf{v}_0(\mathbf{k}')e^{-(s-s_1)(\mathbf{k}-\mathbf{k}')^2-s(\mathbf{k}')^2}d\mathbf{k}'.
\end{aligned} \tag{5}$$

If, as it is assumed in [8], we consider initial data $\mathbf{v}_0$ with a finite support, localized in a sphere around a point $\mathbf{k}^{(0)} \neq 0$, with radius smaller than $|\mathbf{k}^{(0)}|$, we get a simple intuitive representation of the terms of the recursive relation. In fact, the functions $g^{(p)}$ are essentially time integrals of a p-fold convolution of the initial data, so that, by analogy with probability theory, we expect that the support of $g^{(p)}$ is localized around the point $p\mathbf{k}^{(0)}$ with a transversal size which for large p is of the order $\sqrt{p}$. It is then natural to introduce new functions and new variables as follows:

$$\mathbf{k} = p\mathbf{k}^{(0)} + \sqrt{p}\mathbf{Y}, \qquad \mathbf{h}^{(p)}(\mathbf{Y},s) = \mathbf{g}^{(p)}(p\mathbf{k}^{(0)} + \sqrt{p}\mathbf{Y},s), \tag{6}$$

where we can assume $\mathbf{Y} = \mathcal{O}(1)$. (We omit the label (p) if no confusion arises.) If p is large the terms of the sum for $\max\{p_1,p_2\} \leq p^{\frac{1}{2}}$ can be neglected. Moreover the Gaussian densities give a significant contribution only for s_1, s_2 near the endpoint s, so that we introduce new variables $s_j = s(1-\frac{\theta_j}{p_j^2})$, $j = 1,2$, and integrate over θ_j, $j = 1,2$. Setting $\gamma = \frac{p_1}{p}$, and assuming for definiteness $\mathbf{k}^{(0)} = (0,0,a)$, with $a > 0$, we get

$$\mathbf{h}^{(p)}(\mathbf{Y},s) = p^{\frac{5}{2}} \sum_{\substack{p_1+p_2=p\\ p_1,p_2>\sqrt{p}}} \frac{1}{p_1^2p_2^2} \int_{\mathbb{R}^3} P_{\mathbf{e}_3+\frac{\mathbf{Y}}{\sqrt{p}}}\mathbf{h}^{(p_2)}\left(\frac{\mathbf{Y}'}{\sqrt{1-\gamma}},s\right)\cdot \tag{7}$$

$$\cdot\left\langle \mathbf{h}^{(p_1)}\left(\frac{\mathbf{Y}-\mathbf{Y}'}{\sqrt{\gamma}},s\right),\mathbf{e}_3+\frac{\mathbf{Y}}{\sqrt{p}}\right\rangle d\mathbf{Y}'\ (1+o(1)),$$

where $\mathbf{e}_3 = (0,0,1)$ and

$$\mathbf{h}^{(p)}(\mathbf{Y},s) = \left(h_1^{(p)}(\mathbf{Y},s), h_2^{(p)}(\mathbf{Y},s), \frac{F^{(p)}(\mathbf{Y},s)}{\sqrt{p}\,a}\right). \tag{8}$$

The solenoidality condition $\langle \mathbf{h}^{(p)}(\mathbf{Y}, s), \mathbf{k}\rangle = 0$ gives

$$Y_1 h_1^{(p)}(\mathbf{Y}, s) + Y_2 h_2^{(p)}(\mathbf{Y}, s) + F^{(p)}(\mathbf{Y}, s) = \mathcal{O}(p^{-\frac{1}{2}} a^{-1}).$$

Therefore $F^{(p)}(\mathbf{Y}, s)$ is of finite order and the vector $\mathbf{h}^{(p)}(\mathbf{Y}, s)$ is approximately orthogonal to the k_3-axis.

We look for solutions of the recursive relation (7) which for large p are of the form

$$\mathbf{h}^{(p)}(\mathbf{Y}, s) \;=\; p\ (\Lambda(s))^p \prod_{j=1}^{3} g^{(3)}(\mathbf{Y}) \left(\mathbf{H}(\mathbf{Y}) + \delta^{(p)}(\mathbf{Y}, s)\right), \tag{9}$$

where the remainder $\delta^{(p)}$ vanishes as $p \to \infty$, $\Lambda(s)$ is a positive function, which will be discussed below, $g^{(3)}(\mathbf{Y}) = \frac{e^{-\frac{\mathbf{Y}^2}{2}}}{(2\pi)^{\frac{3}{2}}}$ is the standard Gaussian density on $\mathbb{R}^3$, and $\mathbf{H}$ is a vector function independent of time, orthogonal to the k_3-axis, and depending only on Y_1, Y_2: $\mathbf{H}(\mathbf{Y}) = (H_1(Y_1, Y_2), H_2(Y_1, Y_2), 0)$. Proportionality to a Gaussian function is suggested by analogy with the Central Limit Theorem, and it is not restrictive to assume a standard gaussian since the convolution preserves independence of the components and the dispersions can be normalized by rescaling.

In the limit as $p \to \infty$ the sum over p_1 becomes an integral over γ, and after integrating over Y_3, we get a fixed point equation for $\mathbf{H}$ (which, by abuse of notation, is now a vector in $\mathbb{R}^2$)

$$g_1^{(2)}(\mathbf{Y})\mathbf{H}(\mathbf{Y}) = \int_0^1 d\gamma \int_{\mathbb{R}^2} g_\gamma^{(2)}(\mathbf{Y}-\mathbf{Y}') g_{1-\gamma}^{(2)}(\mathbf{Y}') \mathcal{L}(\mathbf{H}; \gamma, \mathbf{Y}, \mathbf{Y}') \mathbf{H}\left(\frac{\mathbf{Y}'}{\sqrt{1-\gamma}}\right) d\mathbf{Y}'. \tag{10}$$

Here $g_\sigma^{(2)}(\mathbf{Y}) = \frac{e^{-\frac{Y_1^2+Y_2^2}{2\sigma}}}{2\pi\sigma}$, and $\mathcal{L}$ is a linear function of $\mathbf{H}$:

$$\begin{aligned}\mathcal{L}(\mathbf{H}; \gamma, \mathbf{Y}, \mathbf{Y}') = -(1-\gamma)^{\frac{3}{2}} \left\langle \frac{\mathbf{Y}-\mathbf{Y}'}{\sqrt{\gamma}}, \mathbf{H}\left(\frac{\mathbf{Y}-\mathbf{Y}'}{\sqrt{\gamma}}\right)\right\rangle + \\ + \gamma^{\frac{1}{2}}(1-\gamma) \left\langle \frac{\mathbf{Y}'}{\sqrt{1-\gamma}}, \mathbf{H}\left(\frac{\mathbf{Y}'}{\sqrt{1-\gamma}}\right)\right\rangle.\end{aligned}$$

The position (9) and the fixed point equation (10) are the basic points of the theory.

In [8] it is proved that there are infinitely many solutions ("fixed points") of the functional equation (10) which can be found by expanding $\mathbf{H}$ in Hermite polynomials He_k, $k = 0, 1, \ldots$. Following [8], we restrict our attention to a particular solution proportional to the radial vector

$$\mathbf{H}^{(0)} = c\ (Y_1, Y_2), \tag{11}$$

where the positive constant c can be obtained by inserting the expression for $\mathbf{H}^{(0)}$ in the fixed point equation (10).

The main result of [8], is the following theorem (in a slightly modified version).

Theorem 1 *For $\mathbf{k}^{(0)} = (0, 0, a)$ and a large enough, there is a 10-parameter set of initial data such that the asymptotic ansatz (9) holds for $\mathbf{H} = \mathbf{H}^{(0)}$ in a non-empty time interval $s \in S = [S_-, S_+]$, with a positive function $\Lambda(s)$, which is strictly increasing, differentiable, and such that $\min_{s\in S} \Lambda'(s) > B > 0$.*

The proof is based on linearized stability analysis, and the renormalization group method. The 10 parameters are related to the components of the unstable and neutral manifold of the linearized map at the fixed point.

The difficult part of the proof is the analysis of the behavior of the remainder, which involves the application of techniques typical of the renormalization group method, and also gives the properties of the function Λ. For the full proofs the reader is referred to [8] and to the references therein.

We now pass to describe the behavior of the blow-up, which in recent years was made more clear by new results, and also by computer simulations. For a more extended discussion we refer to the paper [3].

Observe that the recursive relation (7) and therefore the fixed point equation (10) are unchanged if we replace $\mathbf{h}^{(p)}$ with $(-1)^p\mathbf{h}^{(p)}$. Hence, we have two types of solutions, those for which $h^{(p)}$ is given by (9) (hereafter solutions of type I), and those for which the right side of (9) is multiplied by $(-1)^p$(solutions of type II). If the initial data $\mathbf{v}_0$ leads to a solution of type I with the fixed point $\mathbf{H}^{(0)}$, then the initial data $-\mathbf{v}_0$ lead to a solution of type II with the same fixed point.

Strictly speaking, the proof in [8] holds only for solutions of type I. For solutions of type II observe that by changing the sign of the initial data the behavior of the corrections to the fixed point will be different, leading to a different function Λ. The extension of the proof appears however to be straightforward.

The behavior of the soluttions near the critical time is described by the following proposition, for which we give a sketch of the proof. A more detailed proof is found in [3].

Proposition 2 *If $\mathbf{v}_0$ is chosen as in the above theorem, then by setting $A = \frac{1}{\Lambda(\tau)}$, $\tau \in S$, we obtain a solution that becomes singular at the time $t = \tau$. The total energy and the total enstrophy diverge as*

$$E(t) = \frac{1}{2}\int_{\mathbb{R}^3} |\mathbf{u}(\mathbf{x},t)|^2 d\mathbf{x} = \frac{(2\pi)^3}{2}\int_{\mathbb{R}^3} |\mathbf{v}(\mathbf{k},t)|^2 d\mathbf{k} \sim \frac{C_E^{(\alpha)}}{(\tau - t)^{\beta_\alpha}}, \tag{12}$$

$$S(t) = \int_{\mathbb{R}^3} |\nabla\mathbf{u}(\mathbf{x},t)|^2 d\mathbf{x} = (2\pi)^3\int_{\mathbb{R}^3} \mathbf{k}^2|\mathbf{v}(\mathbf{k},t)|^2 d\mathbf{k} \sim \frac{C_S^{(\alpha)}}{(\tau - t)^{\beta_\alpha+2}}, \tag{13}$$

where $\alpha = I, II$ denotes the type of function, with $\beta_I = 1$, $\beta_{II} = \frac{1}{2}$ and $C_E^{(\alpha)}, C_S^{(\alpha)}$ are constants depending on the initial data.

Moreover the solution $\mathbf{v}(\mathbf{k},t)$ converges point-wise in $\mathbf{k}$ as $t \uparrow \tau$ to a limiting function.

2.1 Sketch of the Proof

For solutions of type I, setting $A = \frac{1}{\Lambda(\tau)}$, for $\tau \in S$, where the interval S is specified in Theorem 1, the tail of the series (4) for $t < \tau$, taking into account (11), is given by the expression

$$\mathbf{v}^{(p_0)}(\mathbf{k},t) = C\sum_{p=p_0}^{\infty} p\ \ g^{(3)}(\mathbf{Y}^{(p)})\ \mathbf{Y}_\perp^{(p)}\int_0^t e^{-\mathbf{k}^2(t-s)}\left(\frac{\Lambda(s)}{\Lambda(\tau)}\right)^p ds, \tag{14}$$

where p_0 is large enough for the asymptotic behavior to set in, $C > 0$ is a constant, and $\mathbf{Y}^{(p)} = \frac{\mathbf{k} - p\mathbf{k}^{(0)}}{\sqrt{p}}$, with $\mathbf{Y}_\perp^{(p)} = (Y_1^{(p)}, Y_2^{(p)}, 0)$.

The asymptotics (14) shows that the main support of the solution extends along the positive k_3-axis in a thin cone of transversal diameter proportional to $\sqrt{k_3}$.

As Λ is strictly increasing, $\frac{\Lambda(s)}{\Lambda(\tau)} < \frac{\Lambda(t)}{\Lambda(\tau)} < 1$, and the terms of the series (14) fall off exponentially fast in p, with an exponential rate which vanishes as $t \uparrow \tau$. Therefore the critical time is τ. By the properties of Λ we have, for $s \uparrow \tau$,

$$\ln \frac{\Lambda(s)}{\Lambda(\tau)} = -\kappa(\tau - s)(1 + r(t - s)), \qquad \kappa = \frac{\Lambda'(\tau)}{\Lambda(\tau)} > 0 \tag{15}$$

where $r(s) \to 0$ as $s \to 0$. Integrating over s, we see that the behavior of the series (14) as $t \uparrow \tau$ is

$$\mathbf{v}^{(p_0)}(\mathbf{k}, t) \sim \text{const} \sum_{p \geq p_0} p \, \frac{e^{-\kappa p(\tau - t)}}{\mathbf{k}^2 + \kappa p} g^{(3)}(\mathbf{Y}^{(p)}) \, \mathbf{Y}_\perp^{(p)} \tag{16}$$

and the L_2-norm is

$$\int_{\mathbb{R}^3} |\mathbf{v}^{(p_0)}(\mathbf{k}, t)|^2 d\mathbf{k} \sim \text{const} \sum_{p_1, p_2 = p_0}^{\infty} \int_{\mathbb{R}^3} \frac{p_1 p_2 e^{-\kappa(p_1 + p_2)(\tau - t)}}{(\mathbf{k}^2 + \kappa p_1)(\mathbf{k}^2 + \kappa p_2)} g^{(3)}$$
$$(\mathbf{Y}^{(p_1)}) \; g^{(3)}(\mathbf{Y}^{(p_2)}) \; \langle \mathbf{Y}_\perp^{(p_1)}, \mathbf{Y}_\perp^{(p_2)} \rangle d\mathbf{k}.$$

A straightforward computation shows that the contribution of the diagonal terms (for $p_1 = p_2$) is of the order $\mathcal{O}((\tau - t)^{-\frac{1}{2}})$. The off-diagonal terms are positively correlated and for a fixed value of p_1 there are $\mathcal{O}((\tau - t)^{-\frac{1}{2}})$ values of p_2 for which the contribution is significant. Therefore the off-diagonal terms give a contribution of order $\mathcal{O}((\tau - t)^{-1})$, which proves relation (12) for $\alpha = I$.

For solutions of type II the asymptotics (16) is modified by inserting an alternating sign $(-1)^p$. The contribution of the diagonal terms has the same form as for $\alpha = I$. For the off-diagonal terms, taking into account the cancellations of neighboring terms, one can see that the total contribution is positive and of the same order as that of the diagonal terms. Hence for $\alpha = II$ the total energy diverges as $(\tau - t)^{-\frac{1}{2}}$.

As for the enstrophy, the estimate is done in the same way as for the energy, except that, because of the factor $\mathbf{k}^2$, the exponent β_α has to be increased by 2.

For point-wise convergence, observe that the series (16) is bounded in absolute value by

$$\text{const} |\mathbf{k}_\perp| \sum_{p = p_0}^{\infty} \frac{p^{\frac{1}{2}}}{\mathbf{k}^2 + \kappa p} \; g^{(3)} \left(\frac{\mathbf{k} - p\mathbf{k}_0}{\sqrt{p}} \right). \tag{17}$$

The terms for $p > \mathbf{k}^2$ are bounded by $C(\mathbf{k}) \; p^{-\frac{1}{2}} \; e^{-\frac{pa^2}{4}}$, where $C(\mathbf{k})$ is a constant depending on $\mathbf{k}$ and the series converges absolutely.

3 Behavior of the Singular Solutions: Computer Simulations and Open Problems

The rigorous results obtained so far leave many open problems on the behavior of the complex solutions near the blow-up, in particular on the picture of the blow-up in x-space and on the dependence of the solutions on the initial data.

In the past few years some significant insight on the behavior of the solutions was obtained from computer simulations performed at the supercomputers of the CINECA center at Bologna (Italy), which are still going on, and are partially reported in [3].

The work at CINECA is based on a new program, written for the simulation of the equations in integral form (2). The program performs very well if one considers that simulating solutions of the Navier–Stokes equations in $\mathbb{R}^3$, and solutions that blow up, is a very challenging task, even for the last generation of supercomputers. A major factor for the success of the program is the relatively simple structure of the solutions in $\mathbf{k}$-space, as we discussed in the previous section. A first attempt to simulate the blow-up of the complex solutions predicted in [8] faced computational difficulties and could only achieve a qualitative description of the divergence of the energy and the enstrophy [1].

The initial data considered for the simulations were of the form

$$\mathbf{v}_0^{\pm}(\mathbf{k}) = \pm\, C \left(k_1, k_2, -\frac{k_1^2+k_2^2}{k_3}\right) \frac{e^{-\frac{(\mathbf{k}-\mathbf{k}^{(0)})^2}{2\sigma^2}}}{(2\pi\sigma^2)^{\frac{3}{2}}}\, g_{\epsilon,\delta}\left(\frac{|\mathbf{k}-\mathbf{k}^{(0)}|}{a}\right), \qquad \mathbf{k}^{(0)} = (0,0,a). \tag{18}$$

Here $a > 0$ is the distance of the center of the support from the origin, the positive constant C controls the initial energy E_0 and the initial enstrophy S_0, and the function $g_{\epsilon,\delta}(r)$, $r \in \mathbb{R}_+$, $1 > \delta > \epsilon > 0$, is a cut-off to avoid the singularity at the origin, which is decreasing, smooth and such that $g_{\epsilon,\delta}(r) = 1$ for $r \le 1-\delta$, and $g_{\epsilon,\delta}(r) = 0$ for $r \ge 1-\epsilon$.

The ratio $\frac{\sigma}{a}$ should be sufficiently small, and in all simulations the cut-off $g_{\epsilon,\delta}$ was replaced by the indicator function of the disk of radius $\delta \in (\frac{1}{2}, 1)$, as the difference was within the computational error.

As we saw, the support of the solution is always contained in the half-space $k_3 > 0$, and is concentrated around the k_3-axis. The discretization in $\mathbf{k}$-space was implemented by a uniform mesh of step 1 contained in the region $R = [-127, 127] \times [-127, 127] \times [-19, L]$, with L between 2028 and 3028. Control simulations with a refined and extended mesh were performed to check stability. The fortunate circumstance that a finer mesh is not needed is due the fact that, as we shall see, the solution $\mathbf{u}(\mathbf{x}, t)$ in $\mathbf{x}$-space is essentially concentrated in a small region around the origin. Most data were collected for $\sigma = 1$, and $15 \le a \le 40$.

The simulations show that if the constant C, is large enough, the initial data (18) generate solutions that blow up with the fixed point (11). Moreover $\mathbf{v}_0^+$ leads to solutions of type I and $\mathbf{v}_0^-$ to solutions of type II.

The blow-up takes place in a very short time. For instance, the solution of type II with $a = 20$ blows up for all C such that $E_0 \ge 25,000$ at a time of the order of 10^{-4} time units (t.u.). Typically the energy decreases for some time, reaching a minimal value after which it starts increasing. The rapid growth of the blow-up takes place in a time of the order of 10^{-5} t.u.

One cannot exclude that solutions with lower values of C blow up at a later time. As the blow-up is very fast, the time step has to be very small, and the simulations at CINECA never went beyond 10^{-2} t.u. The problem whether there is some kind of threshold for the blow-up of solutions with initial data (18) remains open.

Some general features of the solutions near the critical time can be read directly by looking at the tail series (14) and (16), which for solutions of type II are modified by inserting an oscillating factor $(-1)^p$. One can see that the vector field on a plane transversal to the k_3-axis is concentrated in a region of diameter proportional to $\sqrt{k_3}$, and is approximately parallel to the fixed point $\mathbf{H}^{(0)}$. Moreover the modes for large k_3 decrease exponentially fast (with power-law corrections) and the exponential rate decreases in time and vanishes as $t \uparrow \tau$.

The computer simulations show that those features of the solutions set in very early in time, much before the rapid growth of the blow-up, and at moderate values of k_3. In particular they show that the decay along the k_3-axis for large values of k_3 is exponential with great

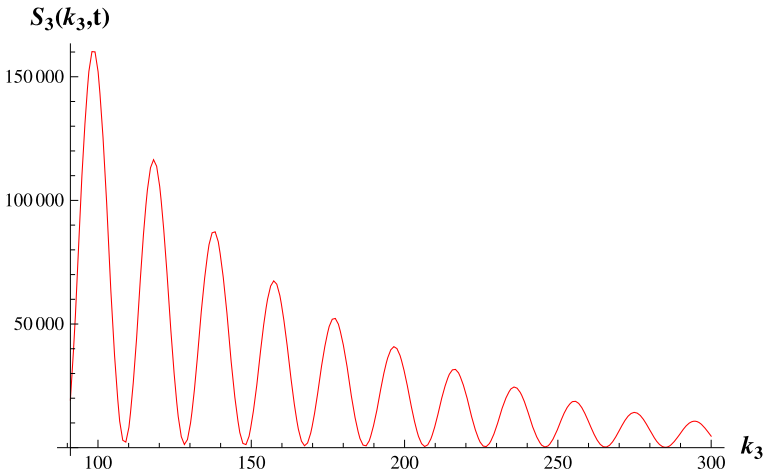

Fig. 1 Plot of the enstrophy marginal density $S_3(k_3, t)$ for the solution of type II at $t = 1125 \times 10^{-7}$ (beginning of the blow-up). The zeroes of the solution are approximately periodic with period $a = 20$

accuracy with a coefficient $\alpha(t)$ which is decreasing in time, and is practically linear in the time range of the blow-up. One can then get a reliable estimate of the critical time τ by taking the intercept of the extrapolation of the graph of $\alpha(t)$ with the horizontal axis $\alpha = 0$.

The behavior of the solutions in **k**-space and in **x**-space, as it comes out of the computer simulations, are well illustrated by plots of the marginal distribution densities of the enstrophy:

$$S_3(k_3, t) = (2\pi)^3 \int_{\mathbb{R}\times\mathbb{R}} |\mathbf{k}|^2 |\mathbf{v}(\mathbf{k}, t)|^2 dk_1 dk_2, \qquad S_1(k_1, t) = (2\pi)^3 \int_{\mathbb{R}\times\mathbb{R}} |\mathbf{k}|^2 |\mathbf{v}(\mathbf{k}, t)|^2 dk_2 dk_3, \tag{19}$$

$$\tilde{S}_3(x_3) = \int_{\mathbb{R}^2} |\nabla \mathbf{u}(\mathbf{x})|^2 \, dx_1 dx_2, \qquad \tilde{S}_1(x_1) = \int_{\mathbb{R}^2} |\nabla \mathbf{u}(\mathbf{x})|^2 \, dx_2 dx_3. \tag{20}$$

By the symmetry of the problem the transversal (with respect to the k_3-axis) marginals $S_2(k_2, t)$, $\tilde{S}_2(x_2, t)$ behave as $S_1(k_1, t)$, $\tilde{S}_1(x_1, t)$.

An important difference between the two types of solutions is that the solutions of type II vanish on the transversal planes $k_3 \approx a(p + \frac{1}{2})$, $p = 1, 2, \ldots$, and in fact, if we fix time and the transversal variables k_1, k_2, the components of $\mathbf{v}(\mathbf{k}, t)$ behave in k_3 as damped oscillations centered at the origin and with approximate period $2a$. The phenomenon is present for all times and extends along the whole simulation range. It is presumably not too hard to obtain a rigorous proof of this kind of behavior based on the alternating signs and a careful analysis of the contribution of the single terms in the series (4).

The damped oscillations of $\mathbf{v}(\mathbf{k}, t)$ in k_3 are well illustrated by the behavior of the marginal density $S_3(k_3, t)$ axis, reported in Fig. 1. The corresponding plot for solutions of type I shows instead only a few oscillations of approximate period a near the origin.

The computer simulations also show that the solutions of type I blow up much earlier than the solutions of type II with the same values of a and C. This fact indicates that, as we mentioned above, the function Λ for the same values of C and a is different in the two cases.

3.1 Dependence on the Initial Data

Some *a priori* indications on the dependence of the blow-up on the initial data comes from the well-known scaling properties of the Navier–Stokes equations in $\mathbb{R}^3$. In fact if λ is a positive parameter, and $\mathbf{v}(\mathbf{k}, t)$ satisfies the equation (2), it is easily seen that the rescaled function

$$\mathbf{v}^{(\lambda)}(\mathbf{k}, t) = \lambda^2 \mathbf{v}(\lambda \mathbf{k}, \frac{t}{\lambda^2}) \tag{21}$$

is also a solution of (2). Therefore if the solution with initial data $\mathbf{v}_0(\mathbf{k})$ blows up at time τ, the solution with the rescaled initial data $\lambda^2 \mathbf{v}_0(\lambda \mathbf{k})$ will blow up at the time $\frac{\tau}{\lambda^2}$. Observe that by rescaling the initial data (18) the parameters σ and a rescale as $\frac{1}{\lambda}$, the initial energy as λ, and the initial enstrophy as $\frac{1}{\lambda}$.

The theory also predicts that if we increase the constant C, which is proportional to the parameter $A = \frac{1}{\Lambda(\tau)}$ in the series (4), then, as Λ is strictly increasing, the critical time τ also increases. By evaluating τ for different values of C and fixed a one can get a detailed information on the function Λ.

Concerning the dependence of τ on a for C fixed, one can guess that if the function Λ does not depend significantly on a, the critical time decreases as a grows, a fact which is well confirmed by the simulations.

A detailed study on the dependence of τ on C and a by computer simulations is in progress.

3.2 Behavior in x-Space: Open Problems

As we saw above, while solutions ot type I have a smooth exponential decay in k_3, the decay of solutions of type II is modulated by an oscillation in k_3 centered at the origin. The picture suggests that the singularities of $\mathbf{u}(\mathbf{x}, t)$, i.e., of the (complex) antitransform of $\mathbf{v}(\mathbf{k}, t)$, are located at $\mathbf{x} = 0$ for solutions of type I and at two singular points $\mathbf{x}_{\pm}^{(0)} = (0, 0, \pm x_3^{(0)})$ with $x_3^{(0)} \approx \frac{\pi}{a}$ for solutions of type II, due to the oscillations in k_3 with approximate period $2a$.

The computer simulations are in full agreement with that prediction. In particular they show for solution of type I a sharp spike of the energy and of the enstrophy at the origin, and for solutions of type II sharp spikes at the points $\mathbf{x}_{\pm}^{(0)}$.

The spikes grow to infinity as $t \uparrow \tau$, and, as expected, the spikes for the enstrophy are sharper than those for the energy. Plots of the marginal densities of the enstrophy $\tilde{S}_3(x_3, t)$ and $\tilde{S}_1(x_1, t)$ are given in Fig. 2 for two values of t near the critical time.

As suggested by Fig. 2, the simulations also show that as $t \uparrow \tau$ the solution $\mathbf{u}(\mathbf{x}, t)$ tends to a finite limiting function everywhere except at $\mathbf{x} = 0$ for type I and $\mathbf{x} = \pm \mathbf{x}^{(0)}$ for type II.

It should be possible to obtain rigorous proofs on the position of the singularities and on the convergence to a limiting function at the critical time, following the same lines as for the analogous results in [9] for the singular complex solutions of the Burgers equations (see also [2] for computer simulations).

4 Concluding Remarks: Some Perspectives on Related Real Flows

The results obtained so far on the behavior of the complex solutions introduced in [8] suggest the application of analogous methods to the study of a related class of real solutions. In fact, if the initial data (18) is antisymmetrized, i.e., if we take as initial data

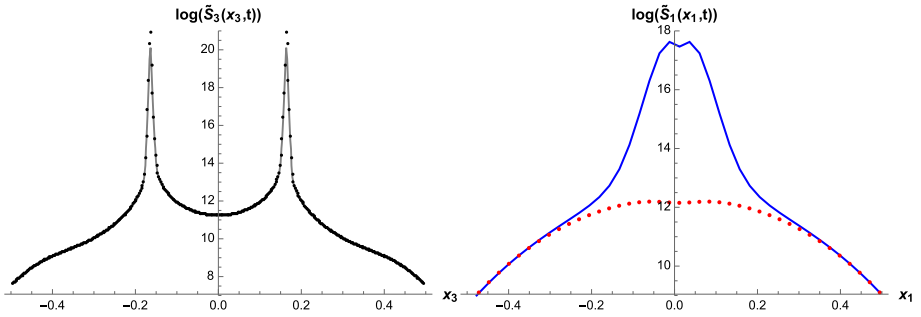

Fig. 2 Type II: Log-plot of the marginal energy densities $\tilde{S}_3(x_3, t)$ (*left*) and $\tilde{S}_1(x_1, t)$ (*right*) at $t \cdot 10^7 = 1521$ (*continuous line*) and $t \times 10^7 = 1544$ (*dotted line*). Longitudinal simulation range $k_3 \in [-19, 2528]$

$$\mathbf{v}_0^{(r)}(\mathbf{k}) = \mathbf{v}_0^{+}(\mathbf{k}) - \mathbf{v}_0^{+}(-k) \tag{22}$$

(the choice $\mathbf{v}_0^{-}$ gives only a change of sign), the solution of Eq. (3) describes a real flow which inherits some basic properties of the complex solutions.

We can again write the power series as in (4), and the recursive relations that follow, except that the term with p convolutions $\mathbf{g}^{(p)}$ is now a sum of terms of different sign, represented as a convolution of $p - j$ factors $\mathbf{v}_0^{+}(\mathbf{k})$ and j factors $-\mathbf{v}_0^{+}(-\mathbf{k})$, for $j = 0, \ldots, p$, with support centered at $(p-2j)\mathbf{k}^{(0)}$. We can however predict that some properties of the complex solutions still hold, in particular that the significant support is concentrated in a thin double cone around the k_3-axis, and that the fixed point $\mathbf{H}^{(0)}$, coming from repeated iterations of $\pm\mathbf{v}_0^{+}(\pm\mathbf{k})$, determines the direction of the flow in $\mathbf{k}$-space.

In absence, so far, of rigorous results, we report some indication coming from computer simulations which were recently done at CINECA, and, as yet, unpublished. The simulations on which we report below were obtained for initial data of the type (22) with $a = 20, 30$ and C large enough (the initial energy is reported in the figure captions).

The simulations show that the velocity field $\mathbf{v}(\mathbf{k}, t)$ aligns to the fixed point $\mathbf{H}^{(0)}$ even for moderate value of k_3 (Fig. 3). Moreover the solution behaves, in analogy with the complex solutions of type II, as a sort of exponentially damped oscillation in k_3 with approximate period $2a$. This is shown by Fig. 4 (left) which gives the behavior of the enstrophy marginal S_3.

The total enstrophy $S(t)$ increases up to a time t_*, after which it decreases. The time t_* and the ratio $R_S = \frac{S_{t_*}}{S_0}$, depend on the initial parameters C and a, and the simulations show that t_* decreases when either C or a increase and R_S increases.

As for the complex case, the solution decays exponentially fast for large k_3 with an exponential rate $\alpha(t)$ that decreases in time, and reaches a minimal value $\bar{\alpha} > 0$ at a time close to t_*, after which it stays more or less constant. Moreover $\bar{\alpha}$ decreases when either C or a increase. We see here a monotonic "worsening" of the analytic properties of the solution $\mathbf{u}(\mathbf{x}, t)$ in time, i.e., a contraction of the radius of convergence of the Taylor series in the space variables.

At the time t_*, when the total enstrophy reaches its maximum, we see that its distribution is concentrated in two spikes, which are located at the same points (or very close to) as for the complex solutions of type II: $\mathbf{x}_{\pm}^{(0)} = (0, 0, \pm x_3^{(0)})$, with $x_3^{(0)} \approx \frac{\pi}{a}$. The phenomenon is illustrated in Fig. 4 (right), which gives a plot of the marginal enstrophy density $\tilde{S}_3(x_3, t)$ close to the time t_*, for $a = 20$, $\frac{\pi}{a} \approx 0.16$.

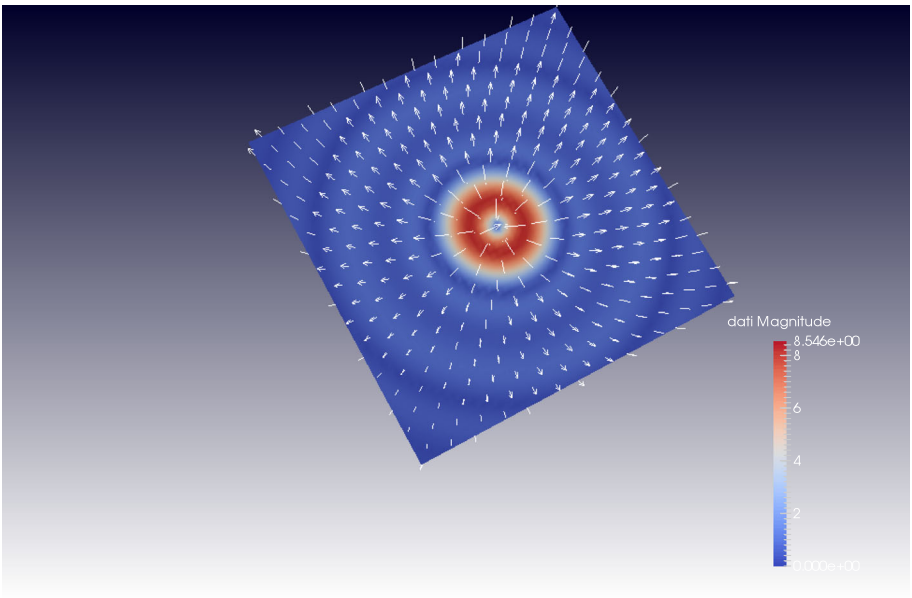

Fig. 3 Real case. initial energy $E_0 = 6.2 \times 10^6$, $a = 20$. $\mathbf{v}(\mathbf{k}, t)$ on the plane $k_3 = 20$, at $t = 500 \times 10^{-7}$, The *arrows* show the direction of the flow at a regular mesh of points. *Dark blue* denotes the region with very low values of the velocity field

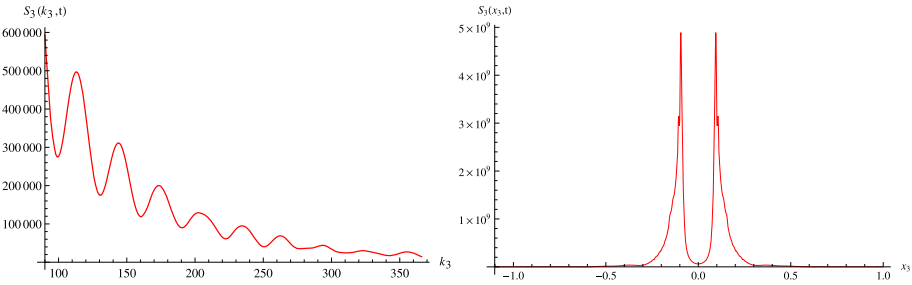

Fig. 4 Real case. initial energy $E_0 = 6.2 \times 10^6$, $a = 20$. *Left* plot of the marginal density $\tilde{S}_3(x_3, t)$ at $t = 1.27 \times 10^{-5}$. *Right* plot of marginal enstrophy density $\tilde{S}_3(x_3, t)$ at $t = t_* = 405 \times 10^{-7}$

More work is under way in order to gain a better understanding by computer simulations of the dependence of the solutions on the initial parameters.

A rigorous analysis with initial data (22) appears to be feasible by refining the methods introduced in [8]. A careful study is needed in order to clarify the role of cancellations which suppress the rapid enhancement of the high k_3-modes shown by the complex solutions, and lead to the limiting exponential decay rate $\bar{\alpha}$. The results are likely to shed more light on the global regularity problem.

Acknowledgements We thank S. Frigio and P. Maponi for many discussions and for providing the data of unpublished computer simulations.

References

1. Arnol'd, M.D., Khokhlov, A.V.: Modeling a blow-up solution of tornado type for the complex version of the three dimensional Navier–Stokes equation. Russ. Math. Surv. **64**, 1133–1135 (2009)
2. Boldrighini, C., Frigio, S., Maponi, P.: Exploding solutions of the two-dimensional Burgers equations: computer simulations. J. Math. Phys. **53**, 083101 (2012)
3. Boldrighini, C., Frigio, S., Maponi, P.: On the blow-up of some complex solutions of the 3-d Navier–Stokes equations: theoretical predictions and computer simulations. (2016) *submitted*
4. Cheskidov, A.: Blow-up in finite time for the dyadic model of the Navier–Stokes equations. Trans. Am. Math. Soc. **10**, 5101–5120 (2008)
5. Hou, ThY: Blow-up or no blow-up? A unified computational and analytic approach to three-dimensional incompressible Euler and Navier–Stokes equations. Acta Numer. **18**, 277–346 (2008)
6. Katz, N., Pavlovic, N.: Finite time blow-up for a dyadic model of the Euler equations. Trans. Am. Math. Soc. **357**, 695–708 (2005)
7. Leray, J.: Sur le mouvement d'un liquide visqueux emplissant l'éspace. Acta Math. **63**, 193–248 (1934)
8. Li, D., Sinai, Y.G.: Blowups of complex solutions of the 3D Navier–Stokes system and renormalization group method. J. Eur. Math. Soc. **10**, 267–313 (2008)
9. Li, D.: Singularities of complex-valued solutions of the two-dimensional Burgers system. J. Math. Phys. **51**, 015205 (2010)
10. Li, D., Sinai, Y.G.: Blowups of complex-valued solutions for some hydrodynamic models. Regul. Chaot. Dyn. **15**(4–5), 521–531 (2010)
11. Seregin, G.: A certain necessary condition of potential blow up for Navier–Stokes equations. Commun. Math. Phys. **312**, 833–845 (2012)
12. Tao, T.: (2016) Finite time blowup for an averaged three-dimensional Navier–Stokes equation. J. Am. Math. Soc. **29**(3), 601–674 (2016)
13. Temam, R.: Navier–Stokes equations. North Holland, Amsterdam (1979)